THE JOURNAL OF BIOLOGICAL CHEMISTRY VOL. 290, NO. 5, pp. 2604–2616, January 30, 2015
© 2015 by The American Society for Biochemistry and Molecular Biology, Inc. Published in the U.S.A.

Mitochondria-associated Endoplasmic Reticulum Membrane (MAM) Regulates Steroidogenic Activity via Steroidogenic Acute Regulatory Protein (StAR)-Voltage-dependent Anion Channel 2 (VDAC2) Interaction*

Received for publication, August 18, 2014, and in revised form, December 2, 2014 Published, JBC Papers in Press, December 10, 2014, DOI 10.1074/jbc.M114.605808

Manoj Prasad[‡1], **Jasmeet Kaur**[‡1], **Kevin J. Pawlak**[‡1], **Mahuya Bose**[§¶1], **Randy M. Whittal**[‖], **and Himangshu S. Bose**[‡**2]

From the [‡]*Mercer University School of Medicine, Savannah, Georgia 31404,* [§]*Center of Excellence for Health Regeneration Biotechnology, Florida Biologix, University of Florida, Alachua, Florida 32615,* [¶]*Department of Physiology and Functional Genomics, University of Florida, Gainesville, Florida 32610,* [‖]*Department of Chemistry, University of Alberta, Alberta T6G2G2, Canada, and* ***Anderson Cancer Institute, Memorial University Medical Center, Savannah, Georgia 31404*

Background: Steroidogenic acute regulatory protein (StAR) fosters cholesterol into the adrenal and gonadal mitochondria to initiate steroidogenesis.
Results: Voltage-dependent anion channel 2 (VDAC2) knockdown ablated pregnenolone synthesis and StAR processing into the mitochondria.
Conclusion: Interaction between StAR and VDAC2 is critical for steroidogenesis.
Significance: VDAC2 is a crucial regulator for initiating steroidogenesis.

Steroid hormones are essential for carbohydrate metabolism, stress management, and reproduction and are synthesized from cholesterol in mitochondria of adrenal glands and gonads/ovaries. In acute stress or hormonal stimulation, steroidogenic acute regulatory protein (StAR) transports substrate cholesterol into the mitochondria for steroidogenesis by an unknown mechanism. Here, we report for the first time that StAR interacts with voltage-dependent anion channel 2 (VDAC2) at the mitochondria-associated endoplasmic reticulum membrane (MAM) prior to its translocation to the mitochondrial matrix. In the MAM, StAR interacts with mitochondrial proteins Tom22 and VDAC2. However, Tom22 knockdown by siRNA had no effect on pregnenolone synthesis. In the absence of VDAC2, StAR was expressed but not processed into the mitochondria as a mature 30-kDa protein. VDAC2 interacted with StAR via its C-terminal 20 amino acids and N-terminal amino acids 221–229, regulating the mitochondrial processing of StAR into the mature protein. In the absence of VDAC2, StAR could not enter the mitochondria or interact with MAM-associated proteins, and therefore steroidogenesis was inhibited. Furthermore, the N terminus was not essential for StAR activity, and the N-terminal deletion mutant continued to interact with VDAC2. The endoplasmic reticulum-targeting prolactin signal sequence did not affect StAR association with the MAM and thus its mitochondrial targeting. Therefore, VDAC2 controls StAR processing and activity, and MAM is thus a central location for initiating mitochondrial steroidogenesis.

The endoplasmic reticulum (ER)[3] and mitochondria are both membrane-bound organelles; however, the ER comprises the nuclear envelope as well as a dynamic peripheral network of tubules and sheets. The ER and mitochondria are physically connected (1) by electron-dense structures (2) forming a protein complex that tethers the two organelles (3), the ER-mitochondrion encounter structure (ERMES). A mammalian phenotype of ERMES is absent. In yeast, mutations in the protein components of the ERMES cause diverse mitochondrial phenotypes, which can be reversed by the expression of the artificial tether (3), suggesting that the main function of the complex is to act as a mechanical link between the ER and mitochondria.

In many mammalian cell types, the ER contains a specialized subdomain, the mitochondria-associated ER membrane (MAM) (2), that physically connects it to the outer mitochondria membrane (OMM) and provides a mitochondrial ER axis that compartmentalizes both stress and metabolic signaling (4, 5). The distance between the ER and OMM was originally estimated to be ~100 nm, but using electron tomography, it was found to be within 10–25 nm (2). The membrane at the ER-mitochondrion junction is tethered by trypsin-sensitive filaments composed of different proteins and lipids (2) and enriched in functionally diverse enzymes involved not only in lipid metabolism but also glucose metabolism (6).

The MAM plays a central role in calcium signaling and phospholipid transport into the mitochondria (6) as a platform for inflammasome signaling, suggesting that it might play a role in

* This work was supported, in whole or in part, by National Institutes of Health Grant HD057876 (to H. S. B.). This work was also supported initially by the American Heart Association and the March of Dimes.
[1] These authors contributed equally to this work.
[2] Supported by the Anderson Cancer Institute. To whom correspondence should be addressed: Dept. of Biochemistry, Division of Biomedical Science, Mercer University School of Medicine and Memorial University Medical Center, Hoskins Research Bldg., 4700 Waters Ave., Savannah, GA 31404. E-mail: bose_hs@mercer.edu and bosehi1@memorialhealth.com.

[3] The abbreviations used are: ER, endoplasmic reticulum; StAR, steroidogenic acute regulatory protein; VDAC, voltage-dependent anion channel; MAM, mitochondria-associated ER membrane; ERMES, ER-mitochondrion encounter structure; OMM, outer mitochondrial membrane; COX IV, *cytochrome-c oxidase IV; BS3, bis(sulfosuccinimidyl)suberate; SCC,* cytochrome P40 side chain cleavage enzyme; DSG, disuccinimidyl glutarate; START, *StAR-related lipid transfer; ERLIN, endoplasmic reticulum lipid raft-associated* protein; PRL, prolactin; GRP, glucose-regulated protein.

infection and immunity (7). The dynamic immune signaling is coordinated by the MAM through membrane-protein interactions governed by mitofusion 2 with membrane tethering sites acting as signaling microdomains (8). Additional proteins found at the interface include the chaperones, calnexin, calreticulin, phosphofurin acidic cluster sorting protein 2, and the σ-1 receptor (3, 6, 9). This σ-1 receptor interacts with voltage-dependent anion channel 2 (VDAC2) to initiate pregnenolone synthesis without affecting steroidogenic acute regulatory protein (StAR) expression (10).

An evolutionarily conserved group of mitochondrially targeted proteins are the β-barrel proteins. These proteins are sorted within the cell and integrated in lipid membranes (11). VDAC is a member of β-barrel membrane proteins (12). This OMM-associated protein allows for the passage of small metabolites, including ATP, across the mitochondrial membranes. VDAC may also mediate hormone-triggered mobilization of cholesterol to the mitochondrial matrix (13), but this has not been proven. The partial amino acid sequence of VDAC (VDAC1 and -2) faces the OMM, and thus it is a part of the MAM region facilitating electrolyte transport and assists in mitochondrial protein sorting (14–16).

Proteins are sorted for translocation across the membrane through recognition of signal sequences. With the exception of a few proteins of the inner membrane and matrix, all mitochondrial proteins are encoded by nuclear genes and are synthesized as precursor proteins on cytosolic polysomes (17). Most matrix proteins carry a positively charged N-terminal presequence that is proteolytically removed after import.

Mitochondrial steroidogenic proteins participate in different steps of steroid hormone synthesis. In an acute response or with hormonal stimulation, StAR is synthesized to transport cholesterol from the OMM to the inner mitochondrial membrane. Although it functions at the OMM, StAR eventually is transported to the mitochondrial matrix as a smaller, mature (30-kDa) protein; its precursor cytoplasmic form is the active form and remains active in a specific conformation induced by cholesterol. However, although the cholesterol transport activity of StAR into mitochondria was identified 20 years ago, the processing mechanism of StAR prior to its import and the role of others factors initiating its activity remain unknown. In this study, we have shown that StAR is first loaded onto the MAM where it interacts with VDAC2 for its processing through the OMM. VDAC2 facilitates StAR processing from a 37- to 32-kDa protein, resulting in its import into mitochondria possibly through the Tom40 channel as a mature 30-kDa protein. In the absence of docking at the MAM, StAR activity is lost, but it can translocate into the mitochondria. Thus, a cascade is formed that is initiated by the proper folding of StAR to its docking to loading onto the mitochondria, which is required for the regulation of steroidogenesis. In summary, the MAM is essential for coordination of cholesterol transport and thus mammalian steroidogenesis.

EXPERIMENTAL PROCEDURES

Reagents and Data Analysis—Antibodies against VDAC1, Tom22, and COX IV were from Santa Cruz Biotechnology or AbCam. P450scc antibody was from ProteinTech (Chicago, IL), rabbit IgG was from Sigma-Aldrich, and protein A beads from Amersham Biosciences/GE Healthcare. Antiserum specific for phospho-StAR was a gift from Dr. Stocco, and all other antibodies were custom synthesized. RNase A and proteinase K were from Roche Applied Science or GE Healthcare. Digitonin was from Calbiochem/EMD Biosciences. Oligonucleotide primers were obtained from Integrated DNA Technology (Ames, IA). Chemical cross-linkers and siRNA were from Life Science (Thermo Fisher, Waltham, MA). All other chemicals were purchased from Sigma-Aldrich unless otherwise specified. All Western blot experiments were performed three times. Most of the figures were generated from the same experiment, and bands were excised from the same autoradiogram, or from two different autoradiograms where the experiments were performed at the same time.

Cell Culture and Transfection—Cell culture, transfections, and mitochondrial isolation from cultured cells were performed following our previously described procedure (18). In some cases, 100 ng/ml trilostane (Steraloids, Los Angeles, CA) was added as an inhibitor of 3β-hydroxysteroid dehydrogenase 2. Mouse Leydig (MA-10) cells were grown in Waymoth medium containing 5% fetal calf serum (FCS) and 10% horse serum supplemented with 1× gentamycin and L-glutamine. For StAR transfection and activity, COS-1 cells were plated at a density of 1×10^6 cells in 6-well plates 24 h prior to transfection followed by co-transfection with 1.0 μg of StAR and F2 (P450scc-adrenodoxin reductase-adrenodoxin) (19) using Lipofectamine (Invitrogen) according to the manufacturer's instructions. COS-1 cells do not express P450scc, so we provided F2 vector, which expresses P450scc, adrenodoxin reductase, and adrenodoxin as a single fusion protein (19) and catalyzes conversion of cholesterol to pregnenolone. The cells were washed with serum-free medium 12 h after transfections and supplemented with medium containing appropriate antibiotics and 10% serum. The medium was collected after 48 h, and the accumulated pregnenolone was measured by radioimmunoassay (RIA kit, MP Biomedicals, Solon, OH). Following transfections of the COS-1 cells with the WT and chimeric constructs, the organelles were fractionated as described later. For metabolic conversion, transfected cells were collected and assayed as described later. For truncated VDAC2 deletional mutants, 1.0 μg of wild type or mutants was transfected with F2 vector following the above procedure.

Animals—Male Sprague-Dawley rats (12 weeks of age) were purchased from Harlan/Sprague-Dawley (Indianapolis, IN) and fed Purina chow (Harlan Teklad Global Diets) and water. Rats weighing 400–450 g were anesthetized with an initial intraperitoneal injection of sodium pentobarbital (40–50 mg/kg) to induce anesthesia. The animals were intubated and mechanically ventilated with oxygen-enriched room air using a rodent respirator (Harvard Rodent Ventilator Model 683). The rate was adjusted to 30–40 breaths/min, and tidal volume was set to 1.1–1.3 ml/100 g of body weight. Procedures for the isolation of adrenal glands and gonads were performed under sterile conditions. The body temperature was maintained at 37 °C by a heating pad.

To isolate the mitochondria from adrenal tissues, the tissues were transferred to mitochondrial isolation buffer (250 mM

sucrose, 10 mM HEPES, 1 mM EGTA, pH 7.4) and chopped into small pieces on ice. Tissue fractions were homogenized in a hand-held all-glass Dounce homogenizer with 10 gentle up and down strokes, and the cell debris was removed by centrifugation at 3,500 × *g* for 10 min. The supernatant containing the mitochondrial fraction was purified by differential centrifugation following a previously reported procedure (20, 21), and the pellet was washed and resuspended in an energy regeneration buffer (125 mM sucrose, 80 mM KCl, 5 mM $MgCl_2$, 10 mM NaH_2PO_4, 10 mM isocitrate, 1.0 mM ATP, 1.0 mM NADP, 0.1 mM ADP, 25 mM HEPES, pH 7.4) prior to storage at either −86 °C or in liquid nitrogen.

Isolation of the Mitochondrial and ER/Mitochondrial Encounter Structure (MAM) Fractions—Steroidogenic MA-10 cells were washed twice with PBS at room temperature, collected by centrifugation at 600 × *g* for 10 min, and then resuspended in 500 μl of 10 mM HEPES, pH 7.4 for 30 min. Next, the cells were diluted further with 800 μl of mitochondrial isolation buffer and homogenized using 45 strokes in an all-glass Dounce homogenizer. The large debris and nuclei were separated by centrifugation twice at 600 × *g* for 10 min. Further centrifugation of the supernatant for 10 min at 10,300 × *g* was performed to isolate the crude mitochondria from the pellet. For the isolation of microsomes, we centrifuged the supernatant at 100,000 × *g* for 1 h. To isolate pure mitochondrial fractions, we resuspended the crude mitochondrial pellet in isolation medium (250 mM mannitol, 5 mM HEPES, pH 7.4, 0.5 mM EGTA, 0.1% BSA) using a Dounce homogenizer to a final volume of 2.0 ml and layered the crude mitochondrial suspension on top of a medium containing density gradient buffer (225 mM mannitol, 25 mM HEPES, pH 7.4, 1 mM EGTA, 0.1% BSA, 30% Percoll (v/v)). After centrifugation at 95,000 × *g* for 30 min, the mitochondrial fraction was isolated two-thirds of the way down the tube, and the ERMES (MAM) complex was found directly above the mitochondrial fraction. The mitochondrial fractions were isolated using a thin Pasteur pipette and washed to remove the Percoll by first diluting them with isolation medium followed by centrifugation twice at 6,300 × *g* for 10 min. The final mitochondrial pellet was resuspended in isolation medium and stored at −86 °C. For isolation of the MAM fraction, the ERMES complex was removed and washed to remove the Percoll by centrifugation at 6,300 × *g* for 10 min followed by further centrifugation of the supernatant at 100,000 × *g*. The resultant MAM fraction was resuspended in 0.5 ml of buffer (0.25 M sucrose, 10 mM Tris-HCl, pH 7.4, 0.1 mM PMSF) and stored at −70 °C.

In Vivo Cross-linking—To study direct interaction of proteins, *in vivo* cross-linking was performed with a major modification of the procedure developed by Selkoe and co-workers (22). MA-10 cells (5×10^6) were grown in tissue cultures dishes, washed twice with PBS at room temperature, and then collected by gentle scraping. Next, the cells were incubated with the cross-linker, BS3 or dithiobis(succinimidyl propionate), which was initially solubilized in DMSO to a working concentration of 50 mM. After incubating the cells with 0.5, 1.0, 2.0, and 5 mM cross-linker at 37 °C for 1 h in a rotating shaker, the reaction was quenched by addition of 1 M Tris, pH 7.6 to a final concentration of 50 mM for an additional 15 min at 4 °C. To avoid any endogenous protease activity, we immediately added a protease inhibitor mixture (Pierce), and incubation continued for an additional 15 min at room temperature. The cross-linked cells were collected by centrifugation at 3,000 rpm and resuspended in 10 mM HEPES, pH 7.4. The organelle fractionation was performed following a standard procedure described previously (21, 23).

StAR Import Assays—[^{35}S]Methionine (Met)-labeled StAR and SCC/StAR were synthesized in a cell-free system using a TNT rabbit reticulocyte system (Promega, Madison, WI). Ribosomes and their associated polypeptide chains were removed by centrifugation at 150,000 × *g* for 15 min at 4 °C as described previously (24). For all protein import experiments, 100 μg of isolated mitochondria was incubated in a 26 °C water bath with ^{35}S-labeled StAR or ^{35}S-labeled SCC/StAR to a final volume of 100 μl, and the reaction was terminated by the addition of 1 mM carbonyl cyanide *m*-chlorophenylhydrazone and an equal volume of boiling 2× SDS sample buffer. The import reactions were analyzed by SDS-PAGE, fixed in methanol/acetic acid (40:10), dried, and exposed to a phosphorimaging screen.

Organelle Fractionation and ER Association of Chimeric Proteins—Cell-free transcription/translation synthesis (cell-free system) of the specific chimeric cDNAs was performed to express proteins for *in vitro* experiments using wheat germ extract (Promega) labeled with [^{35}S]methionine (MP Biomedicals). The wheat extract provides ribosomes and cofactors for protein expression. The cDNAs of interest coupled to an SP6 promoter were added along with SP6 polymerase (Promega) in the presence and absence of rough microsomal membranes from dog pancreas (1 μl of rough microsomal membranes/12.5 μl of translational reaction was added). The mixture was incubated at 22 °C for 2 h, separated by SDS-PAGE, and visualized through phosphorimaging or by autoradiography. The figures were prepared from the same experiment or two identical experiments performed at two different times without changing the integrity of the figure.

An aliquot of translated protein was used to collect rough microsomal membranes with ultracentrifugation at 109,000 × *g* (Beckman TL-100.2) at 4 °C for 30 min. The supernatant was collected, and the pellet was treated with freshly prepared 100 mM sodium carbonate solution, pH 11.4 on ice for 15 min. The samples were ultracentrifuged to separate the soluble fraction from the membranous fraction. Soluble fractions were pooled together. As a control, the pellet was washed with buffer. After separation by SDS-PAGE, all radioactive bands were visualized through phosphorimaging and by autoradiography.

Immunoprecipitation Analysis—Digitonin extracts from mitochondria incubated with ^{35}S-labeled StAR were immunoprecipitated overnight at 4 °C with the indicated antibodies (Santa Cruz Biotechnology, AbCam, custom synthesized, or kind gifts from scientists) in 25 mM Tris-HCl, pH 7.5, 1% Triton X-100, 0.5% Nonidet P-40, 200 mM NaCl, 0.5% sodium-deoxycholate, 0.01–0.03% SDS, 1× protease inhibitor mixture. StAR preimmune serum was added as a negative control, and StAR antiserum was added as a positive control. Protein A-Sepharose CL-4B (GE Healthcare/Amersham Biosciences) was used to isolate the immunocomplexes, which were eluted by boiling for 15 min in 1× SDS sample buffer and analyzed by SDS-PAGE.

Purification and Identification of Complexes by Two-dimensional Native PAGE—Proteins were first separated in 3–16% native gels. After the region containing the StAR-associated complex was excised, it was re-electrophoresed vertically in a 3–16% gradient native gel under identical conditions overnight at 4 °C. The gel was fixed in methanol/acetic acid (40:10), dried, and exposed to x-ray film. The corresponding exposed regions were excised and processed for mass spectrometric analysis.

Density Gradient Ultracentrifugation—Complexes were resolved by a sucrose density gradient (top 10% to bottom 30%) with a cushion of 200 μl of 68% (2.0 M) sucrose to a final volume of 2 ml. Approximately 100 μg of protein in 100 μl was layered on the top and centrifuged at 4 °C in a Beckman TLA55 rotor at 55,000 rpm for 4 h. After centrifugation, fractions of 125 μl were collected. Gradient fractions were analyzed by native PAGE to show that the complexes were not degraded during the sucrose density gradient resolution and subjected to immunoprecipitation to determine StAR-specific interaction. An aliquot of 20 μl of each fraction was analyzed via 15% SDS-PAGE; the same volume was processed for immunoprecipitation and Western blot analyses.

Chemical Cross-linking—Isolated MAM fractions were incubated with various concentrations BS3 or disuccinimidyl glutarate (DSG) solubilized in DMSO. For DMSO solubilization of cross-linkers, first a stock concentration was made, and then it was gradually diluted to a final working concentration of 1 or 10 mM that was prepared in the NaH_2PO_4 or HEPES buffer. The reactions were terminated either by transferring them on ice or by the addition of ~10–20 μl of 1.0 M Tris buffer, pH 9.0 depending on the experimental requirement.

siRNA Knockdown and Metabolic Conversion—We used the same sequence for knocking down Tom22 as described before (23). To knock down the VDAC2 expression, MA-10 or COS-1 cells were incubated with 30 or 60 pmol of siRNA (5′-GGGAGUGUAUAAACCUCGG-3′ and 5′-CCGAGGUUUAUACACUCCC-3′) for 24, 36, and 48 h after which target protein expression was determined by Western blotting with specific antibodies. Conditions that yielded at least 80% knockdown were used for subsequent analyses. For metabolic conversion, 20 μg of mitochondrial protein or cell lysate was incubated with NADPH for evaluation of cholesterol to pregnenolone conversion. For quantitative analysis of each steroid synthesized, radioactive spots on the silica plates were scraped, and the silica was extracted with a solvent mixture of ether/chloroform (3:1). After the solvent was evaporated under N_2, the extract was brought up in 100 μl of MeOH, and then radioactive counts were determined.

VDAC2 Antibody Production—To have a pure VDAC2-specific antibody, we synthesized a 51-mer peptide matching the human VDAC2 sequence (NH_2-YQLDPTASISAKYQLDPTASISAKVVYQLDPTASISAKYQLDPTASISAKC-COOH) from P_i Proteomics, LLC (Huntsville, AL). The purified peptide was then sent to an antibody company (Lampire Biologicals, Coopersburg, PA) for conjugation with keyhole limpet hemocyanin and ovalbumin to obtain rabbit polyclonal antibodies. The project was initiated with two rabbits that received a booster at every 3rd week for a period of 87 days. Once the antibody titer reached more than 1:5,000 by Western blot analysis, the rabbits were exsanguinated, and the whole serum was stored as 1 ml at −86 °C. A small aliquot of 1.0 ml was stored at −20 °C for immediate use.

Mass Spectrometry—The stained protein bands were excised, destained, reduced with DTT (Roche Applied Science), alkylated with iodoacetamide (Sigma), and digested with trypsin (Promega sequencing grade modified) overnight as described previously (50). The resulting peptides extracted from the gel were analyzed via LC-MS/MS on a nanoAcquity UPLC (Waters) coupled with a Q-ToF-Premier mass spectrometer (Micromass/Waters). Tryptic peptides were separated using a linear water/acetonitrile gradient (0.1% formic acid) on a nanoAcquity column (3-μm Atlantis dC_{18}, 100-Å pore size, 75-μm inner diameter × 15 cm) with an in-line Symmetry column (5-μm C_{18}, 180-μm inner diameter × 20 mm; Waters) used as a loading/desalting column. Proteins from the generated MS/MS spectra were identified by searching the NCBI nonredundant database using Mascot MS/MS Ion Search (Matrix Science) with consideration for carbamidomethylated cysteine and oxidation of methionine.

RESULTS

Segregation of Proteins into the MAM Region—Cholesterol transport is crucial for steroidogenesis. Cholesterol cannot be directly transported into the mitochondria; it requires lipid membranes as a carrier, and thus a connection between the ER and mitochondria (*i.e.* MAM) is necessary. In mammals, nonvesicular cholesterol transport across organelles is facilitated by lipid transfer proteins known to bind sterols, including START domain-containing proteins (25). Although it is known that StAR fosters cholesterol into the mitochondria, its mechanism of processing is unknown. START domain-containing proteins are active outside of the mitochondria (26, 27). StARD3 is 50% active after deletion of the N terminus; however, StARD6 is active even without a mitochondrial targeting sequence. Therefore, we hypothesized that despite the membrane continuity by the MAM further translocation and maintenance of network activity require appropriate protein conformation.

To understand the role of the MAM in cholesterol trafficking to mitochondria for steroidogenesis, we purified it from testicular tissues through Percoll density gradient centrifugation. After digitonin solubilization, the main constituents were identified first by native gradient PAGE followed by mass spectrometric analysis. As shown in Fig. 1*A*, we found two closely related StAR-containing complexes of 500 and 290 kDa. The presence of multiple protein complexes is likely due to the effects of MAM tethering, which tends to occur in clusters of six or more, incrementally spaced 13–22 nm apart spanning distances of 6–15 nm (1).

The 500-kDa band was excised and subjected to mass spectrometric analysis (LC-MS/MS), which revealed the presence of several proteins (Table 1) that were identified by Mascot MS/MS Ion Search against the NCBI (non-redundant) database, including mitochondrial, MAM, and ER-associated proteins. The mitochondrial proteins included Tom22, VDAC2, and StAR, and the ER-associated proteins included calnexin, glucose-regulated protein (GRP) 78, ERLIN-2, and solute carrier protein (SLC). The 290-kDa complex contained most of the

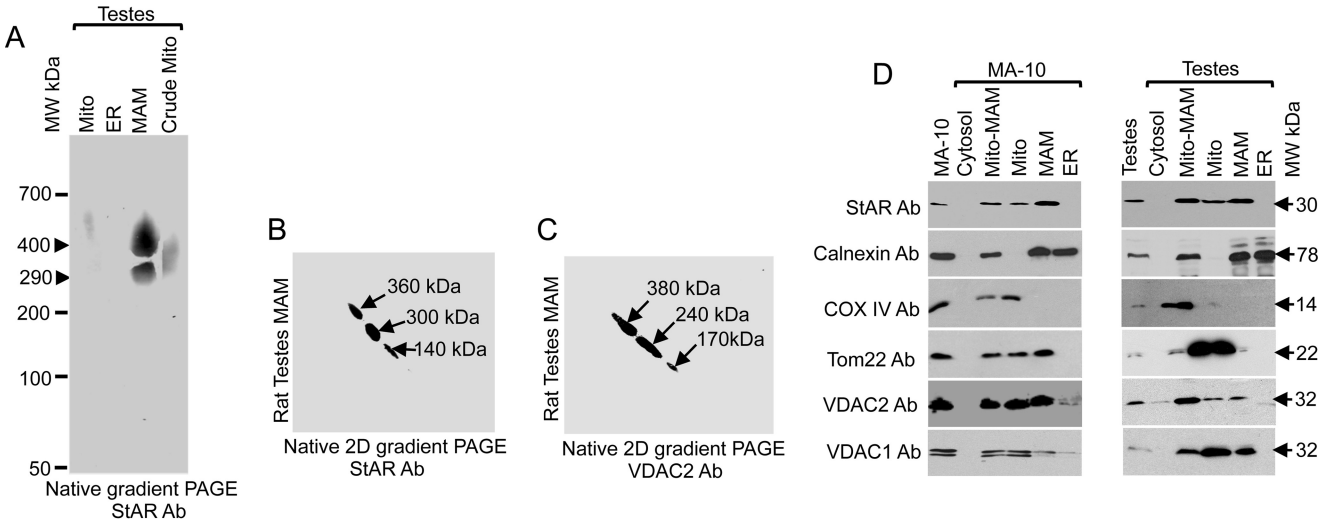

FIGURE 1. **Characterization of MAM-associated proteins.** *A*, native gradient PAGE of rat testis subcellular fractions probed with an anti-StAR antibody (*Ab*). *B* and *C*, two-dimensional (*2D*) native PAGE of the high molecular weight complex excised out from the one-dimensional native PAGE stained with StAR (*B*) and VDAC2 (*C*) antibodies independently. *D*, MAM, ER, crude mitochondrial (*Mito-MAM*), and cytosolic fractions isolated from MA-10 cell and rat testicular fractions probed with the indicated antibodies. *Mito*, mitochondria.

TABLE 1

One-dimensional native gel (3–16%) PAGE of the mitochondria-associated membrane fraction isolated from rat testes (Complex 1 from Fig. 1A; 500 kDa)

Accession no.	Protein	No. of unique peptides
25742763	GRP78	9
25282419	Calnexin	7
148747140	Solute carrier family 2	4
38512106	Ribophorin	13
149023097	Protein-disulfide isomerase	1
13786202	VDAC2	6
62078695	Malectin	2
149029483	ATP synthase	7
157823984	ERLIN-2	11
157822157	ERLIN-1	3
11177910	HSP70	7
238336	3βHSD2	6
4558732	VDAC1	2
25742763	Tom22	2
52630888	StAR	2
2257955	Cytochrome b_5	2

TABLE 2

One-dimensional native gel (3–16%) PAGE of the mitochondria-associated membrane fraction isolated from rat testes (Complex 2 from Fig. 1A; 290 kDa)

Accession no.	Protein	No. of unique peptides
25742763	GRP78 (ER)	12
25282419	Calnexin	7
148747140	Solute carrier family 2	7
38512106	Ribophorin	7
149023097	Protein-disulfide isomerase	4
13786202	VDAC2	1
62078695	Malectin	2
149029483	ATP synthase	7
210032365	Endoplasmin precursor	5
157822989	Calmegin precursor (ER chaperone; testis)	8
2257955	Cytochrome b_5	1

MAM-associated proteins as identified in Table 1, excluding StAR and ERLINs (Table 2). The presence of StAR was always detected by Western blotting, but by mass spectrometric analysis, it was detected in less than 50% of the MAM fractions, suggesting that it was possibly masked by another abundantly expressed MAM protein or that most of the protein was processed to mature mitochondrial protein (28). The identification of chaperones suggests the formation of lipid raftlike domains that facilitate the processing of signal peptides and thus possibly facilitate the formation of the MAM (29, 30). It is likely that these chaperones mediate the association of other proteins to form a tether, which may affect steroidogenic activity.

To identify additional sheet-segregating proteins that could potentially be more strongly and preferentially associated with the StAR-containing protein complex and are required for StAR interaction and targeting to the mitochondrial membrane, we reasoned that such proteins would maintain a strong interaction with a flexible organelle, such as the mitochondria, and that proteins with a weaker interaction would be lost. Thus, we excised the band from the one-dimensional native gradient PAGE and subjected it to two-dimensional native gradient PAGE (31) followed by Western blotting with antibodies specific for StAR and VDAC2. The presence of StAR and VDAC2 (Fig. 1, *B* and *C*, respectively) was observed. In two-dimensional native PAGE, the StAR-containing complex was separated into three complexes of 360, 300, and 140 kDa in size, suggesting that the large complex is composed of three smaller complexes (Fig. 1*B*). Similar results were observed for VDAC2 (Fig. 1*C*). The abundance of StAR and VDAC2 at the same location is suggestive of a possible interaction between these two proteins. We excised the specific 240- and 380-kDa complexes from the two-dimensional native PAGE and subjected them to mass spectrometric analysis. As shown in Tables 3 and 4, GRP78 and other ER-associated proteins were present; however, StAR and VDAC2 were absent in the two-dimensional PAGE possibly due to loose association with the main 500-kDa complex (Table 1). VDAC2 is exposed toward the cytoplasm (14), facilitating the interaction between cytoplasmic proteins or proteins at the border of the cytoplasm and mitochondria.

To confirm the presence of these proteins in the specific cellular fractions, we subjected mouse Leydig MA-10 cells and testicular tissues to subcellular fractionation followed by Western blotting with specific antibodies. Because of the similarity in

TABLE 3

Two-dimensional native gel (3–16%) PAGE of the mitochondria-associated membrane fraction isolated from rat testes (Complex 1 from Fig. 1C; 380 kDa)

Accession no.	Protein	No. of unique peptides
25742763	GRP78 (ER)	14
25282419	Calnexin	8
210032365	Endoplasmin precursor	26
148747140	Solute carrier family 2; facilitated glucose transporter 3	4
157822989	Calmegin precursor	6
23477364	11β-Hydroxysteroid dehydrogenase 1	2
52345385	Protein-disulfide isomerase	2
51859516	HSP90 (cytosolic)	6
56090325	Transmembrane protein 206	2

TABLE 4

Two-dimensional native gel (3–16%) PAGE of the mitochondria-associated membrane fraction isolated from rat testes (Complex 2 from Fig. 1C; 240 kDa)

Accession no.	Protein	No. of unique peptides
25742763	GRP78 (ER)	7
25282419	Calnexin	7
210032365	Endoplasmin precursor	4
148747140	Solute carrier family 2; facilitated glucose transporter 3	3
157822989	Calmegin precursor	4
23477364	11β-Hydroxysteroid dehydrogenase 1	2
52345385	Protein-disulfide isomerase	2
149036687	Ribophorin 1	2

electrophoresis pattern of the isolated MAM and mitochondria from the adrenal and testicular tissues, we have presented only testicular tissues. As shown in Fig. 1*D*, StAR was observed predominately in the MAM fraction of gonads as well as MA-10 cell fractions. VDAC2 was present in the mitochondria, MAM, and crude mitochondrial fractions (Fig. 1*D*). These data suggest that mitochondrial StAR transits through the MAM where it interacts with multiple ER- and mitochondria-associated proteins for cholesterol fostering. Therefore, transport of StAR to mitochondria was possibly successful due to the mitochondria-associated outer membrane connecting multiple proteins at one time.

VDAC2 Interaction with the MAM—Steroidogenic activity and cholesterol transport are dependent on the stability and expression of StAR as well as the availability of the active protein at the OMM as only newly synthesized StAR can foster cholesterol (26). We hypothesize that OMM-associated VDAC2 interacts with the MAM-associated StAR, targeting it toward the appropriate compartment in a manner different from other translocases as VDAC2 requires a continuous interaction with the MAM. Thus, we examined the StAR-VDAC2 interaction in more detail. To evaluate the proximity of StAR with MAM proteins, we performed *in vitro* chemical cross-linking with BS3, which has an 11.4-Å spacer, immediately after isolation of the MAM from rat adrenal glands. StAR-associated cross-linked complexes were identified by immunostaining with StAR (Fig. 2*A*, *left-hand panel*) and VDAC2 antibodies (Fig. 2*A*, *right-hand panel*) and confirmed by mass spectrometric analysis. First a newly generated cross-linked ~80-kDa band and then a 140-kDa protein band were observed (Fig. 2*A*). We next excised the bands and subjected them to mass spectrometric analysis, which also identified StAR and VDAC2 in the 140-kDa band. These results were confirmed by immunoprecipitation of the cross-linked rat testis MAM fractions with StAR (Fig. 2*B*) and VDAC2 (Fig. 2*C*) antibodies. To confirm our *in vitro* cross-linking results, we next performed co-immunoprecipitation with different antibodies. As a control, we included rat IgG, biosynthetic StAR, and COS-1 cells (Fig. 2*D*). The results confirmed that StAR interacted with VDAC2 (Fig. 2*D*).

Next, we purified the digitonin-solubilized complex through sucrose density gradient purification and determined the localization of the MAM-associated proteins in various fractions using the indicated antibodies (Fig. 2*E*). After 1 h of centrifugation, 37-kDa StAR (Fig. 2*E*, *panel a*) and 32-kDa StAR (Fig. 2*E*, *panel b*) were detected; however, after 4-h centrifugation, the amount of 37- and 32-kDa StAR in fraction 10 increased. The displayed profile of a quick move from fraction 3 to fraction 10 by StAR suggests a possible loose association with the interacting proteins. VDAC2 fractionated at a location similar to that of StAR from fractions 4 to 12. However, the VDAC2 band intensity was higher than that of StAR (Fig. 2*E*, *panel c*). After 4 h of centrifugation, VDAC2 moved marginally from fractions 4 through 8 to fraction 13, which is similar to that of 32-kDa StAR (Fig. 2*E*, *panel a*); therefore, it is likely that the 32-kDa StAR associated with VDAC2 to a greater extent than did the 37-kDa StAR. This is possibly because VDAC2 has a longer N-terminal region than VDAC1, and deletion of 20 amino acids from the N terminus reduced VDAC2 activity by more than 30% (32), shifting the channel into a closed state.

In Vivo Interaction of VDAC2 with StAR—To understand whether the interaction of StAR with VDAC2 is necessary for steroidogenesis, we stimulated MA-10 cells with cAMP and performed *in vivo* chemical cross-linking of whole cells with various concentrations of the chemical cross-linkers BS3 and dithiobis(succinimidyl propionate) (Fig. 3, *A–D*). The cross-linked cells were then solubilized with digitonin and analyzed by Western blotting with VDAC2, StAR, Tom22, and COX IV antibodies independently. Interaction between VDAC2 and StAR was initiated with 0.5 mM cross-linker, and band intensity was increased with increasing cross-linker concentrations, decreasing again with ≥5 mM cross-linker (Fig. 3, *A–D*). The top 135-kDa band is the newly generated cross-linked product, and the bottom band is that of the specific protein, confirming that StAR interacted with VDAC2 only (Fig. 3*A*). However, this same analysis with VDAC2 (Fig. 3*B*) antibodies showed an 80-kDa band and a more pronounced 135-kDa band, which may represent the pool of protein that is integrated with the OMM (Fig. 3*B*). Identical results were observed when probing with Tom22 antibody (Fig. 3*C*). The 135-kDa protein band was absent after probing with antibodies specific for the matrix-resident COX IV (Fig. 3*D*). To confirm the specificity of *in vivo* cross-linking, we immunoprecipitated the cross-linked product with the StAR and VDAC2 antibodies (Fig. 3, *E* and *F*). Both antibodies pulled out the high molecular weight band, confirming that StAR interacts with VDAC2.

VDAC2 Regulates StAR Processing—The MAM-associated StAR co-localized with mitochondrial VDAC2 and Tom22 either all at once or one at a time. To determine whether interaction with any of these proteins determines the fate of StAR, we first silenced VDAC2 expression and then determined StAR

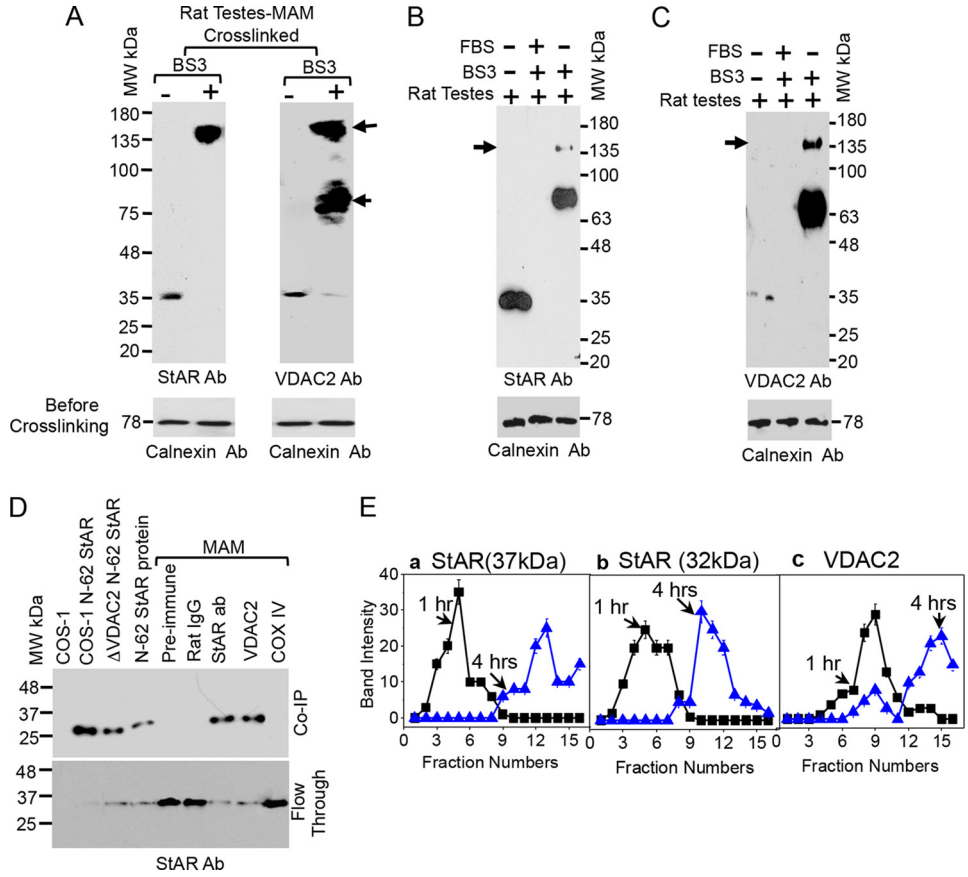

FIGURE 2. **Interaction of VDAC2 with StAR.** *A*, chemical cross-linking of the purified rat testis MAM with BS3 followed by Western blotting with StAR and VDAC2 antibodies independently. *B* and *C*, identification of the MAM-interacting proteins. Purified MAM was incubated with the chemical cross-linker BS3, immunoprecipitated, and then analyzed by Western blotting independently with the indicated antibodies. Fetal bovine serum (FBS) was used as a negative control to show the specificity of StAR and VDAC2 antibodies. *D*, co-immunoprecipitation (*Co-IP*) of the indicated antibodies followed by Western blotting with a StAR antibody (*Ab*). *E*, *panels a–c*, determination of the localization of the different MAM-associated proteins of rat testes using sucrose density gradient analysis of the digitonin-lysed mitochondrial complexes after 1 (*solid squares*) and 4 (*solid triangles*) h of ultracentrifugation. Each fraction was probed with the indicated antibodies, and the distribution of the proteins was graphed. Data presented are the mean ± S.E. (*error bars*) of three independent experiments. StAR was associated for a limited time of 1 h with all the MAM-associated proteins analyzed. The *bottom panels* are the Western blots prior to cross-linking showing an equivalent loading in each lane.

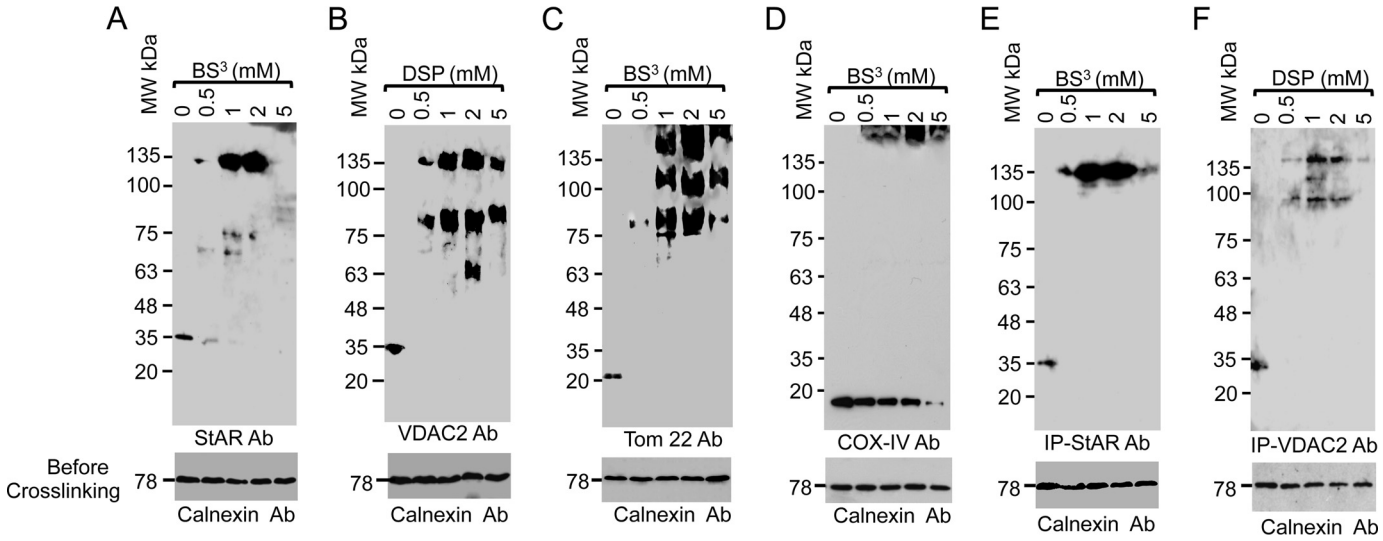

FIGURE 3. ***In vivo* interaction of StAR with VDAC2.** *A–D*, *in vivo* chemical cross-linking of the MA-10 cells with BS3 or dithiobis(succinimidyl propionate) (*DSP*) and identification of the chemically cross-linked protein bands by Western staining with the StAR (*A*), VDAC2 (*B*), Tom22 (*C*), and COX IV (*D*) antibodies. The *bottom panels* in *A–D* show the Western staining of the same cross-linked reaction prior to cross-linking with calnexin antibody (*Ab*) showing that the starting amount of lysate in each experiment was identical. *E* and *F*, immunoprecipitation (*IP*) of the *in vivo* cross-linked product (shown in *A* and *B*) with StAR (*E*) and VDAC2 (*F*) antibodies. The *bottom panel* is the Western staining with calnexin antibody of the total cell lysate prior to immunoprecipitation.

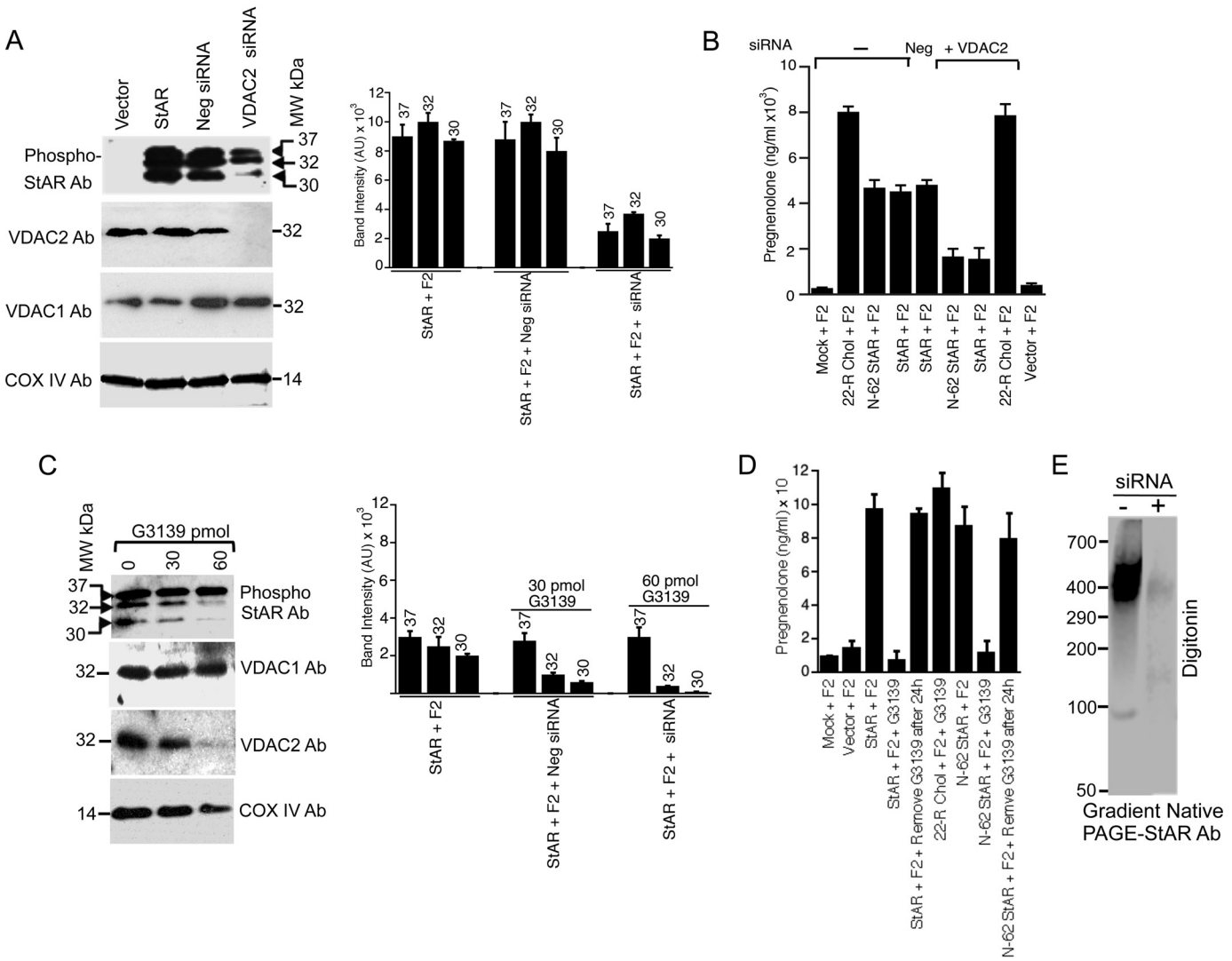

FIGURE 4. **Role of VDAC2 in steroidogenesis.** *A*, expression of StAR in COS-1 cells after transfection with full-length StAR and VDAC2 knockdown. Processing of 30-kDa StAR was inhibited in the absence of VDAC2. The *right-hand panel* shows the quantitative measurement of the intensity of Western blotting with the ImageQuant program showing the level of expression after VDAC2 knockdown with siRNA. *AU*, arbitrary units; *Neg*, negative. Data in *A* are expressed as the mean ± S.E. of three separate experiments, each performed in triplicate. *B*, measurement of pregnenolone synthesis after overexpression of full-length or N-62 StAR in MA-10 cells with and without VDAC2 knockdown by VDAC2 siRNA. 22(*R*)-Hydroxycholesterol (*22-R Chol*) was used in the incubation as a positive control. *C*, expression of full-length StAR after inhibiting VDAC2 expression with G3139. The *bottom panels* are the Western blots with the indicated antibodies after VDAC2 knockdown showing that VDAC1 expression was unaffected. The *right-hand panel* shows similar quantitative measurement of the intensity of bands as performed in *A*. *D*, measurement of pregnenolone synthesis with and without incubation of 60 pmol of G3139 after transfection of full-length or N-62 StAR. Also in one lane, G3139 was removed from the cells 24 h after incubation. 22(*R*)-Hydroxycholesterol was used in the incubation as a positive control. *E*, after digitonin solubilization, ΔVDAC2 cell extracts were separated by native gradient PAGE and stained with a StAR antibody (*Ab*), which showed the absence of a StAR complex. Data in *A*–*D* are expressed as the mean ± S.E. (*error bars*) of three separate experiments, each performed in triplicate at a different time.

expression in various subcellular fractions. As shown in Fig. 4*A*, in the absence of VDAC2, primarily 37- and 32-kDa StAR was detected with very little mature 30-kDa StAR, suggesting that the majority of StAR was not imported into the mitochondria. Knocking down VDAC2 also had no effect on VDAC1 and COX IV expression (Fig. 4*A*, *bottom panels*). A quantitative estimation of the intensity of the bands is presented in the *right-hand panel* (Fig. 4*A*). To confirm that the reduced expression of mature 30-kDa StAR was related to the absence of VDAC2 expression, we next measured the cholesterol levels in wild-type and ΔVDAC2 cells by measuring the amount of pregnenolone synthesis after transfection with StAR cDNA as described previously (15, 18, 33). As expected, compared with parental cells, ΔVDAC2 cells had reduced cholesterol transport and thus lower pregnenolone synthesis (Fig. 4*B*). Next, the effect of the VDAC2 inhibitor G3139 on StAR fate was determined. G3139 is a 31-mer phosphorothioate oligonucleotide that stops VDAC2 expression without inhibiting VDAC1 expression (34). As shown in Fig. 4*C*, incubation with 60 pmol of G3139 ablated VDAC2 expression, which also reduced the levels of mature phosphorylated StAR, suggesting that in the absence of VDAC2 processing of StAR was inhibited. In contrast, the expression of VDAC1 or COX IV was not inhibited by G3139 (Fig. 4*C*). We determined the intensity of the bands before and after incubation of G3139 (Fig. 4*C*, *right-hand panel*). To confirm that indeed VDAC1 and VDAC2 work independently, we performed a metabolic conversion assay with the mitochondria isolated from stable MA-10 cells in which VDAC1 and VDAC2

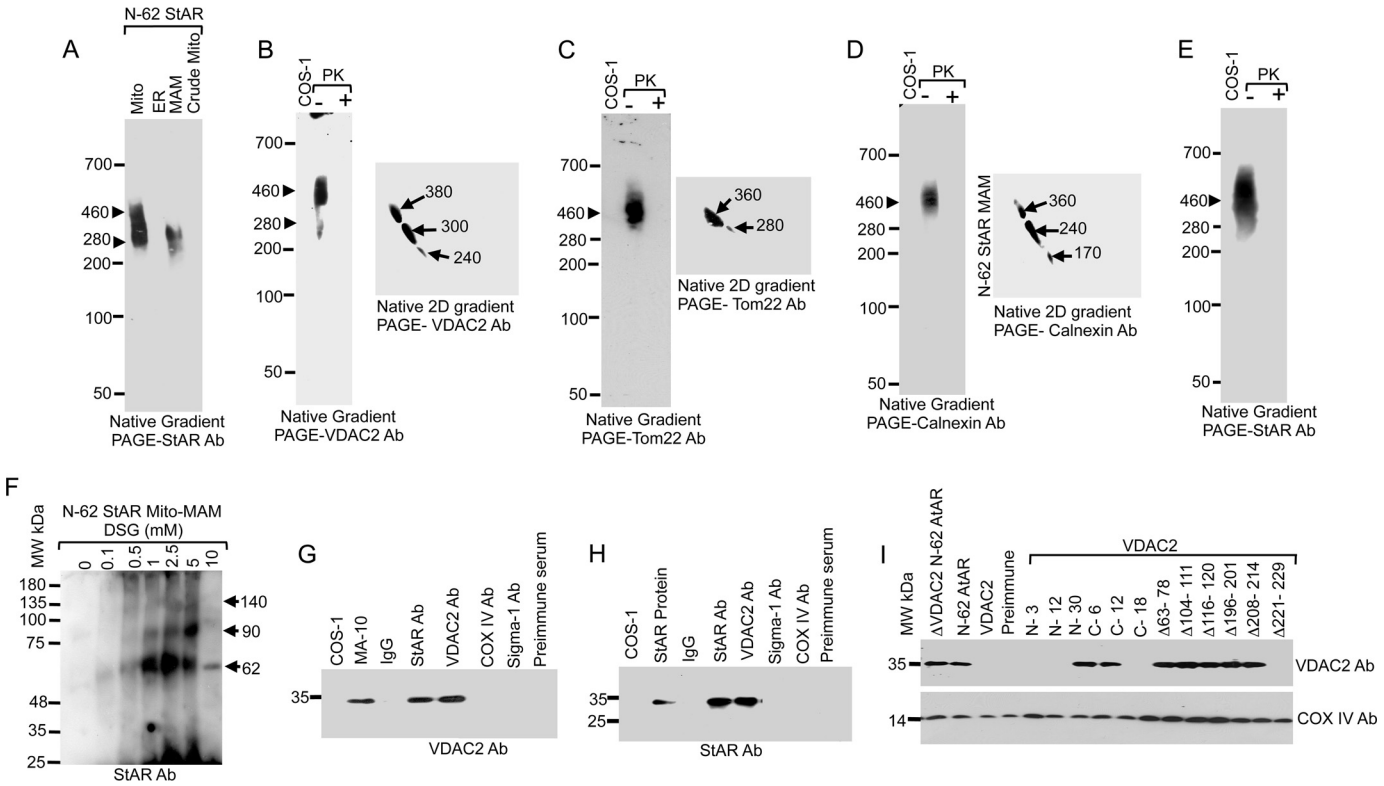

FIGURE 5. **StAR translocation in the absence of its own N-terminal sequence.** *A*, analysis of cellular fractions by native gradient PAGE in COS-1 cells overexpressing N-62 StAR and probed with the StAR antibody (*Ab*). *B–D*, identification of the MAM-associated proteins of COS-1 cells that overexpress N-62 StAR. The MAM fractions were analyzed by one-dimensional native gradient PAGE followed by two-dimensional (*2D*) analysis of the excised band from the one-dimensional native PAGE. The identity of the complexes was visualized after staining with the indicated antibodies. *E*, analysis of the MAM fractions by native gradient PAGE with and without incubation with proteinase K (*PK*) and staining with a StAR antibody. *F*, the MAM fraction of N-62 StAR-expressing cells was cross-linked with increasing concentrations of the chemical cross-linker DSG, separated by SDS-PAGE, and stained with a StAR antibody. Three cross-linked products of 62, 90, and 140 kDa band were identified. The MAM fraction was immunoprecipitated with the indicated antibodies and blotted with VDAC2 (*G*) and StAR (*H*) antibodies. *I*, ΔVDAC2 COS-1 cells overexpressing N-62 StAR were transfected with the indicated VDAC2 deletion mutants, immunoprecipitated with a StAR antibody, and immunoblotted with a VDAC2 antibody. Deletion of more than 18 amino acids from the C terminus ablated VDAC2 interaction with StAR, and similarly the region of amino acids 221–229 was equally important, but deletion of any amino acids from the first N-terminal sequence ablated interaction with StAR. The *bottom panels* probed with COX IV antibody show as equivalent amount of protein present in each lane. *Mito*, mitochondria; *Mito-MAM*, crude mitochondria.

siRNAs are expressed (ΔVDAC1 and ΔVDAC2, respectively). To confirm the complete absence of 30-kDa StAR and minimal expression of 32-kDa StAR after incubation with 60 pmol of G3139, we determined the activity after transfecting COS-1 cells with full-length and N-62 StAR. The pregnenolone synthesis was completely ablated in the presence of G3139 and was restored when G3139 was removed from the cells (Fig. 4*D*). Digitonin solubilization of the mitochondrial fraction isolated from MA-10 cells followed by native PAGE and probing with a StAR antibody revealed a 500-kDa complex that was absent in ΔVDAC2 MA-10 cells (Fig. 4*E*), suggesting that in the absence of VDAC2 the mitochondrial StAR was minimal. These experiments demonstrate that StAR processing requires VDAC2 at the OMM, and thus the inner mitochondrial membrane- and intermembrane space-resident enzyme activity is not affected. These results further explain the importance of VDAC2 and illustrate that StAR is active prior to its import into mitochondria.

Mechanism of StAR Activation in the Absence of its N-terminal Sequence—Previous studies have shown that StAR is active after deletion of its N-terminal 62-amino acid sequence (35, 36). To determine whether the N-terminal deleted StAR is either in the cytoplasm or acting at the mitochondria (35) or MAM, we fractionated N-62 StAR-expressing stable cells. After native gradient PAGE and Western blotting with antibodies specific for StAR, we found that most of the protein remained in the mitochondrial fraction with a small amount at the MAM (Fig. 5*A*). Further probing of crude mitochondrial extracts showed that the StAR-containing complexes were of a similar size as that observed for VDAC2, Tom22, and calnexin. Moreover, the interaction of the VDAC2- (Fig. 5*B*), Tom22- (Fig. 5*C*), calnexin- (Fig. 5*D*), and StAR (Fig. 5*E*)-containing complexes was not coordinately linked as they were proteolyzed with as little as 100 ng/ml of proteinase K (Fig. 5*E*). Mass spectrometric analysis of the proteins from one-dimensional and two-dimensional PAGE identified similar MAM-associated proteins (Table 5). Two-dimensional native PAGE of N-62 and Western blot staining with StAR were similar to Fig. 1*B* (data not shown). Thus, in the absence of the N-terminal sequence, StAR was not lost in the cytoplasm but was associated with the crude mitochondrial fraction.

To characterize the interaction among the proteins in the MAM region, we performed chemical cross-linking of the MAM fraction of N-62 StAR-expressing cells using a homobifunctional membrane-permeable cross-linker (DSG) that cross-links through amine-reactive *N*-hydroxysuccinimide

TABLE 5

One-dimensional native gel (3–16%) PAGE of the mitochondria-associated membrane fraction isolated from N-62-expressing COS-1 cells (Complex 1 from Fig. 5A; 460 kDa)

PCP, phosphate carrier protein.

Accession no.	Protein	No. of unique peptides
386758	GRP78	14
109080088	Calnexin	8
297265432	Protein-disulfide isomerase	4
109078796	HSP70	8
355748592	HSP90	3
4507677	Endoplasmin	9
25188179	VDAC2	3
109078605	VDAC1	4
355558313	Sodium/potassium ATPase	3
297268779	Serpin H1 (HSP47) serine protease inhibitor	3
297298293	Transmembrane protein TMP21	1
109122310	ERGIC-53 lactose-mannose-binding 1	2
355566443	Mitsugumin 23 (ER transmembrane; 23 kDa)	1
355564589	PCP precursor	1
355563339	Diacylglycerol synthase	1

esters at both ends of a five-atom (7.7-Å) spacer arm. The cross-linked products were stained with StAR antibody. As shown in Fig. 5*F*, a band of 62 kDa was observed with 0.5 mM DSG, and this band increased in intensity with increasing concentration of DSG up to 5 mM after which it decreased. Other less intense bands of 90 and 140 kDa were also observed with 1 mM DSG. Next, subsequent co-immunoprecipitation analysis of the MAM region confirmed the interaction with VDAC2 (Fig. 5, *G* and *H*). We expect that regions of VDAC2 facing the cytoplasm are responsible for its interaction with N-62 StAR. Based on the model structure for VDAC2, which suggests a fundamentally β-barrel structure (14, 37), the possible sites that mediate this interaction include 30 amino acids from the N terminus and 30 amino acids from the C terminus. VDAC1 and VDAC2 have 72% amino acid identity, and thus the model structure shows that exposure of internal amino acid regions to the cytoplasmic side of the mitochondria from amino acids 63–78, 104–111, 116–120, 196–201, 208–214, and 221–229 may facilitate the interaction with the MAM. Therefore, we determined the interaction of each of these regions by overexpressing VDAC2 deletion constructs in cells with stable VDAC2 knockdown and StAR expression. As shown in Fig. 5*I*, immunoprecipitation with a StAR antibody followed by Western blotting with a VDAC2 antibody showed that deletion of VDAC2 N-terminal amino acids (N-3, N-12, and N-30) ablated its interaction with StAR. Alternatively, the N-terminal amino acids may be buried within the membrane and not available for interaction with StAR. Deletion mutants of 12 or fewer amino acids from the C terminus (C-6 and C-12) continued to interact with StAR. However, the interaction was lost with deletion of 18 C-terminal amino acids (C-18; Fig. 5*I*).

A model structure of the N- and C-terminal regions, which might be facing the mitochondrial *intermembrane* space, is not available at present. Therefore, we constructed various internal deletion mutants of VDAC2 and assessed their ability to interact with StAR. As shown in Fig. 5*I*, the Δ221–229 VDAC2 mutant failed to interact with StAR, suggesting that the N terminus and the C terminus at or after 18 amino acids as well as amino acids 221–229 are required for VDAC2 interaction with StAR.

Specificity of StAR Targeting from the MAM to the Mitochondria—StAR import is slower than that observed for other mitochondrial targeting sequences (18), and it competes only with its own N-terminal sequence (38); however, the impact of the N-terminal sequence is unknown. Therefore, we constructed a recombinant StAR in which 30 amino acids of the N-terminal StAR sequence were substituted with the P450scc mitochondrial sequence (SCC/StAR) and determined whether it still transits through the MAM fraction. As shown in Fig. 6*A*, SCC/StAR was present in the ER, MAM, and mitochondrial fractions. However, no localization in the MAM fraction was detected after deletion of the 32-amino acid pause sequence between amino acids 30 and 62 of StAR (ΔPause StAR; Fig. 6*A*), suggesting that this region is responsible for directing StAR through the MAM. Probing the same membrane with an anti-VDAC2 antibody showed its localization in the crude and pure mitochondrial fractions as well as at the MAM; calnexin was only in the ER fraction, confirming the purity of the fractionation.

Because SCC/StAR remains in the MAM fraction, we replaced the first 31 amino acids of StAR with the ER-targeting N-terminal 31 amino acids of prolactin (PRL), a secretory protein with an ER-targeting signal sequence that is cleaved between amino acids 30 and 31 (39). As shown in Fig. 6*B*, PRL(1–31)-StAR was processed in a fashion identical to that observed for wild-type StAR, indicating that the PRL signal sequence did not affect its processing prior to entry into the mitochondria. Chimeric proteins in which the first 30 or 62 amino acids of StAR were replaced with the 31-amino acid PRL signal sequence were expressed at sizes similar to that of wild-type StAR (Fig. 6*B*). However, the reverse construction where StAR(1–30) was fused with PRL(1–229) did not localize to the mitochondria, suggesting that the C terminus of StAR is required for its mitochondrial targeting (Fig. 6*B*, *top panel*). Probing the same membrane with an anti-PRL antibody revealed only the full-length PRL (Fig. 6*B*, *middle panel*). Therefore, we next performed organelle fractionation and observed that wild-type StAR with its own N-terminal sequence was imported into the mitochondria (Fig. 6*C*). Similarly, the fusion of ER signal sequence prior to the full-length StAR led to direct import into the mitochondria, confirming the specificity of the StAR N-terminal sequence (Fig. 6*D*). However, fusions with the ER signal sequence replacing either the first 30 (Fig. 6*E*) or 62 (Fig. 6*F*) amino acids of StAR resulted in the protein not being targeted fully to ER. Most of the expressed protein remained associated with the OMM. Electron microscopic (35) and biochemical (36) experiments by two different groups showed that the localization of the N-terminal deleted StAR remained near the OMM. Western staining of the organelle fractionation with VDAC2 showed its presence at the mitochondria; similarly, calnexin was present only in the ER, confirming the accuracy of our organelle fractionation. In summary, we have confirmed the specificity of StAR mitochondrial targeting where the C terminus is essential for mitochondrial association at the OMM and thus steroidogenic activity (18, 40).

To confirm the above observation that the C-terminal region of StAR targeted mitochondria, we placed the PRL signal

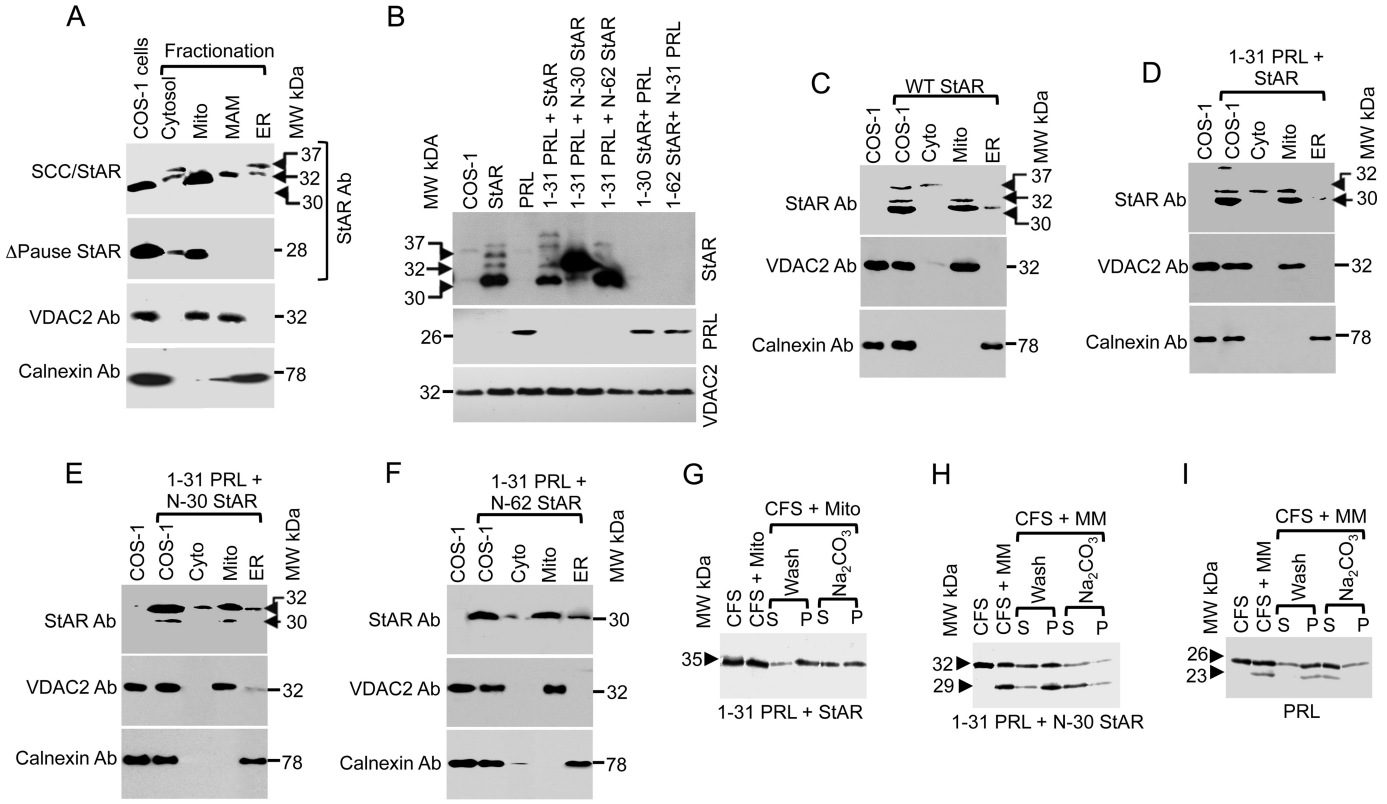

FIGURE 6. **Specificity of StAR signal sequence recognition.** *A*, subcellular localization of chimeric [^{35}S]methionine-labeled SCC/StAR in which 30 amino acids of the N terminus were substituted with the matrix-targeted fusion protein SCC. The fusion protein still targets to the ER and MAM first and then to the mitochondria (*top panel*). Deleting the pause sequence (amino acids 31–62) of StAR inhibits its transit to the ER or MAM (*second panel*). The *bottom panels* validate the purity of fractionation using the mitochondrial marker VDAC2 and ER marker calnexin. *B*, StAR processing fusion with the ER targeting signal sequence of PRL analyzed by Western blotting with a StAR antibody (*Ab*). The commercially available PRL antibody recognized only the full-length protein (*bottom panel*). The same membrane was probed with a VDAC2 antibody to validate that the same amount of protein was present in each lane. *C*, organelle fractionation of the overexpression of full-length StAR in COS-1 cells. The compartmental fractions were confirmed by mitochondrial (VDAC2) and ER (calnexin) antibodies (*bottom panels*). *D--F* are the StAR fusion proteins fractionated after overexpression in a fashion similar to that shown in *C*. *G*, confirmation of the import of [^{35}S]methionine-labeled cell-free synthesized fusion proteins (PRL(1–31)-StAR) into the mitochondria and integration analysis by sodium carbonate extraction where the fusion protein remained in the pellet (*P*). The unimported supernatant is denoted by "*S*," and the imported pellet fraction is denoted by "*P*." *H*, the ER-targeting of [^{35}S]methionine-labeled co-translation of PRL(1–31)- N-30 StAR with the microsomal membrane and its analysis before and after extraction with carbonate. *I*, [^{35}S]methionine-labeled cell-free synthesis of PRL with the microsomal membrane and extraction of the imported fraction with carbonate showing that the N-terminal sequence was cleaved after processing through the microsomal membrane and remained as a soluble ER protein. *Mito*, mitochondria; *MM*, microsomal membrane; *CFS*, cell-free system.

sequence prior to the N terminus of StAR, expecting that this fusion would also be transported. We translated the PRL(1–31)-StAR fusion protein in a cell-free system in the presence of isolated mitochondria from MA-10 cells. PRL-StAR targeting to the mitochondria was observed despite the presence of the PRL signal sequence (Fig. 6*G*). After carbonate extraction, the majority of the protein remains in the pellet because sodium carbonate breaks the protein-protein interaction but not the lipid-protein interaction (41). The first 30 amino acids of StAR might be responsible for its mitochondrial import. To confirm that indeed the PRL(1–31)-N-30 StAR did not target to the mitochondria, we synthesized it in the presence of microsomal membranes where this fusion protein undergoes processing to form the lower molecular mass protein (28 kDa), and it was mostly concentrated in the pellet fraction. However, it was recovered in the soluble fraction after carbonate fraction (Fig. 6*H*), suggesting that the PRL signal sequence was processed in the ER, and then the protein remained in the ER lumen (Fig. 6*H*) similar to full-length PRL (Fig. 6*I*) (42). In summary, these results confirm that amino acids 31–62 of StAR are required for its association with the MAM, and the N-terminal sequence only facilitates mitochondrial targeting.

DISCUSSION

The MAM has emerged as an ER domain enriched with numerous chaperones and oxidoreductases (43), suggesting that a targeting mechanism exists for these proteins. Within the smooth ER, calnexin accumulates on the MAM.

Cholesterol is the precursor of all steroids, and its uptake by lipoproteins accounts for more than 80% of adrenal cholesterol. The direction of cholesterol flux in the adrenal glands and gonads is dependent upon the state of the organism. In the basal or resting state, cholesterol storage and efflux predominate. During an acute stress response, the immediate need for mitochondrial cholesterol is accompanied by the rapid mobilization of intracellular cholesterol stores. Chronic stress, either environmental or dietary, results in the sustained import of cholesterol into the cell and mitochondria. Basal storage of cholesterol in the form of cholesterol esters is maintained primarily through the action of acetyl-CoA:cholesterol esterase. Under

stress, the flux of cholesterol changes dramatically due to enhanced hydrolysis of stored cholesterol esters, increased uptake of plasma cholesterol, and transport of free cholesterol into the mitochondria for the synthesis of steroid hormones in response to ACTH. Free cholesterol induces tighter StAR folding; however, excess cholesterol results in the unfolding of StAR (38). Thus, in the presence of excess cholesterol, StAR may possibly remain associated with the other MAM proteins, and after most of the cholesterol pool is imported into the mitochondria, the remaining cholesterol may promote StAR refolding. Because StAR has a mitochondrial leader sequence and thus does not covalently remain associated with the other identified proteins, it remains close enough to the mitochondrial membrane that it is eventually transported into the mitochondria.

Although the role of the MAM in connecting the mitochondria and ER has been well characterized, the role of specific MAM-associated proteins in the formation of its characteristic tethering was unknown. In the present study, a strong interaction of MAM-associated StAR with VDAC2 and Tom22 was observed. The tethering initiates with the cytoplasmic proteins, which remain in the dimeric state and are possibly assisted by chaperones to ensure the proper folding of StAR.

Because StAR is responsible for fostering cholesterol into the mitochondria, the presence of chaperones at the MAM region possibly helps in the proper folding of StAR and therefore steroidogenesis. Calcium stimulates steroidogenesis in adrenal cells (44), and the MAM-associated chaperone GRP78 is a Ca^{2+}-binding protein. Therefore, it is possible that an induction of GRP78 is required to block ER stress signals, maintain ER function and integrity, ensure protein folding, and protect cells from misfolded protein toxicity (45). Thus the proteins at the MAM possibly require a master chaperone for folding and activity.

The uncoupling protein response is a highly conserved signaling pathway activated when an accumulation of luminal unfolded protein exceeds ER folding capacity in a sudden or acute condition or upon hormonal stimulation. StAR is expressed in acute conditions, and thus a master regulator chaperone of the uncoupling protein response (46, 47) would be essential for its appropriate folding, which is required for its targeting to the mitochondria. StAR has a mitochondrial targeting sequence, and its import is slower than that of other mitochondrial targeting proteins (18, 38). In the absence of proper folding, StAR would be proteolyzed by the proteasomal protease (15).

Partially unfolded StAR is the most active form prior to its entry into the mitochondria (18, 40), and thus StAR remains at the MAM. During its transient residency at the MAM, it requires interaction with the σ-1 receptor (10), which facilitates interaction with the VDAC2. In non-steroidogenic COS-1 cells, VDAC2 knockdown reduced progesterone synthesis by more than 80%. Inhibition of VDAC2 by G3139 also suppressed the processing of StAR. The N-terminal sequence of StAR targets it to the MAM, and during density gradient centrifugation, StAR and VDAC2 were fractionated similarly, forming endogenous complexes in rat adrenal glands and testes. However, the mitochondrial import of SCC/StAR was 4 times faster than that of StAR (18) with the majority of the protein being targeted to mitochondria with a minor portion associated with the MAM and ER. Furthermore, a series of experiments with StAR-PRL fusion proteins revealed that amino acids 31–62 of StAR are required for its association with the MAM, and the N-terminal sequence only facilitates mitochondrial targeting. Taken together, these results suggest that steroidogenic protein transit through the MAM is required for initiating their targeting to the mitochondrial membrane.

The presence of the StAR pause sequence (amino acids 31–62) is essential for interactions with the VDAC2, which in turn retains it at the OMM for a longer time, thus increasing cholesterol fostering capacity into the mitochondria (18, 40). In the absence of the pause, StAR was imported directly without the need for chaperones for its folding and interaction with the VDAC2, resulting in no or very little pregnenolone synthesis (Fig. 4*D*). In the absence of pause, SCC/N-62 StAR was imported 4 times faster than StAR (18). The interaction of VDAC2 with StAR is likely with amino acids 221–229 and the C-terminal 20 amino acids (Fig. 5*I*). Like the new class of β-barrel proteins (11, 12, 16), the C-terminal 30 amino acids of VDAC are facing the cytoplasm, facilitating the interaction with the StAR pause sequence. StAR folding is crucial for interaction and activity (33, 48, 49). In the absence of StAR interaction with VDAC2, the unimported and possibly misfolded protein is proteolyzed by the proteasomal proteases (15). In summary, VDAC2 regulates StAR mitochondrial import, ultimately helping pregnenolone synthesis and maintaining steroidogenic activity.

Acknowledgments—We are thankful to Dr. Vishwanath R. Lingappa from the University of California, San Francisco for the Sp6 vector and for signal sequence peptides and Dr. Douglas M. Stocco for the phospho-StAR antibody. We are extremely thankful to Dr. Robert Brown from Genta Inc. for the G3139 oligonucleotide.

REFERENCES

1. Mannella, C. A., Buttle, K., Rath, B. K., and Marko, M. (1998) Electron microscopic tomography of rat-liver mitochondria and their interaction with the endoplasmic reticulum. *BioFactors* **8,** 225–228
2. Csordás, G., Renken, C., Várnai, P., Walter, L., Weaver, D., Buttle, K. F., Balla, T., Mannella, C. A., and Hajnóczky, G. (2006) Structural and functional features and significance of the physical linkage between ER and mitochondria. *J. Cell Biol.* **174,** 915–921
3. Kornmann, B., Currie, E., Collins, S. R., Schuldiner, M., Nunnari, J., Weissman, J. S., and Walter, P. (2009) An ER-mitochondria tethering complex revealed by a synthetic biology screen. *Science* **325,** 477–481
4. Vance, J. E. (1990) Phospholipid synthesis in a membrane fraction associated with mitochondria. *J. Biol. Chem.* **265,** 7248–7256
5. Lebiedzinska, M., Szabadkai, G., Jones, A. W., Duszynski, J., and Wieckowski, M. R. (2009) Interactions between the endoplasmic reticulum, mitochondria, plasma membrane and other subcellular organelles. *Int. J. Biochem. Cell Biol.* **41,** 1805–1816
6. Hayashi, T., Rizzuto, R., Hajnoczky, G., and Su, T. P. (2009) MAM: more than just a housekeeper. *Trends Cell Biol.* **19,** 81–88
7. Zhou, R., Yazdi, A. S., Menu, P., and Tschopp, J. (2011) A role for mitochondria in NLRP3 inflammasome activation. *Nature* **469,** 221–225
8. Horner, S. M., Liu, H. M., Park, H. S., Briley, J., and Gale, M., Jr. (2011) Mitochondrial-associated endoplasmic reticulum membranes (MAM) form innate synapses and are targeted by hepatitis C virus. *Proc. Natl. Acad. Sci. U.S.A.* **108,** 14590–14595

9. Simmen, T., Aslan, J. E., Blagoveshchenskaya, A. D., Thomas, L., Wan, L., Xiang, Y., Feliciangeli, S. F., Hung, C. H., Crump, C. M., and Thomas, G. (2005) PACS-2 controls endoplasmic reticulum-mitochondria communication and Bid-mediated apoptosis. *EMBO J.* **24,** 717–729
10. Marriott, K. S., Prasad, M., Thapliyal, V., and Bose, H. S. (2012) σ-1 receptor at the mitochondrial associated ER-membrane is responsible for mitochondrial metabolic regulation. *J. Pharmacol. Exp. Ther.* **343,** 578–586
11. Paschen, S. A., Waizenegger, T., Stan, T., Preuss, M., Cyrklaff, M., Hell, K., Rapaport, D., and Neupert, W. (2003) Evolutionary conservation of biogenesis of β-barrel membrane proteins. *Nature* **426,** 862–866
12. Paschen, S. A., Neupert, W., and Rapaport, D. (2005) Biogenesis of β-barrel membrane proteins of mitochondria. *Trends Biochem. Sci.* **30,** 575–582
13. Jefcoate, C. (2002) High-flux mitochondrial cholesterol trafficking, a specialized function of the adrenal cortex. *J. Clin. Investig.* **110,** 881–890
14. Colombini, M. (2012) VDAC structure, selectivity, and dynamics. *Biochim. Biophys. Acta* **1818,** 1457–1465
15. Bose, M., Whittal, R. M., Miller, W. L., and Bose, H. S. (2008) Steroidogenic activity of StAR requires contact with mitochondrial VDAC1 and phosphate carrier protein. *J. Biol. Chem.* **283,** 8837–8845
16. Hiller, S., Garces, R. G., Malia, T. J., Orekhov, V. Y., Colombini, M., and Wagner, G. (2008) Solution structure of the integral human membrane protein VDAC-1 in detergent micelles. *Science* **321,** 1206–1210
17. Herrmann, J. M., and Neupert, W. (2000) Protein transport into mitochondria. *Curr. Opin. Microbiol.* **3,** 210–214
18. Bose, H. S., Lingappa, V. R., and Miller, W. L. (2002) Rapid regulation of steroidogenesis by mitochondrial protein import. *Nature* **417,** 87–91
19. Harikrishna, J. A., Black, S. M., Szklarz, G. D., and Miller, W. L. (1993) Construction and function of fusion enzymes of the human cytochrome P450scc system. *DNA Cell Biol.* **12,** 371–379
20. Bose, M., Adams, B. P., Whittal, R. M., and Bose, H. S. (2008) Identification of unknown protein complex members by radiolocalization and analysis of low-abundance complexes resolved using native PAGE. *Electrophoresis* **29,** 753–760
21. Bose, M., Debnath, D., Chen, Y., and Bose, H. S. (2007) Folding, activity and import of steroidogenic acute regulatory protein (StAR) into mitochondria changed by nicotine exposure. *J. Mol. Endocrinol.* **39,** 67–79
22. Dettmer, U., Newman, A. J., Luth, E. S., Bartels, T., and Selkoe, D. (2013) *In vivo* cross-linking reveals principally oligomeric forms of α-synuclein and β-synuclein in neurons and non-neuronal cells. *J. Biol. Chem.* **288,** 6371–6385
23. Pawlak, K. J., Prasad, M., Thomas, J. L., Whittal, R. M., and Bose, H. S. (2011) Inner mitochondrial translocase Tim50 interacts with 3β-hydroxysteroid dehydrogenase type-2 to regulate adrenal and gonadal steroidogenesis. *J. Biol. Chem.* **286,** 39130–39140
24. Schwartz, M. P., and Matouschek, A. (1999) The dimensions of the protein import channels in the outer and inner mitochondrial membrane. *Proc. Natl. Acad. Sci. U.S.A.* **96,** 13086–13090
25. Holthuis, J. C., and Levine, T. P. (2005) Lipid: traffic: floppy drives and a super highway. *Nat. Rev. Mol. Cell Biol.* **6,** 209–220
26. Miller, W. L., and Bose, H. S. (2011) Early steps in steroidogenesis: intracellular cholesterol trafficking. *J. Lipid Res.* **52,** 2111–2135
27. Bose, H. S. (2011) Mechanistic sequence of mitochondrial cholesterol transport by StAR proteins. *J. Proteins Proteomics* **2,** 1–9
28. Stocco, D. M., and Clark, B. J. (1996) Regulation of the acute production of steroids in steroidogenic cells. *Endocr. Rev.* **17,** 221–244
29. Browman, D. T., Resek, M. E., Zajchowski, L. D., and Robbins, S. M. (2006) Erlin-1 and erlin-2 are novel members of the prohibitin family of proteins that define lipid-raft-like domains of the ER. *J. Cell Sci.* **119,** 3149–3160
30. Kammoun, H. L., Chabanon, H., Hainault, I., Luquet, S., Magnan, C., Koike, T., Ferré, P., and Foufelle, F. (2009) GRP78 expression inhibits insulin and ER stress-induced SREBP-1c activation and reduces hepatic steatosis in mice. *J. Clin. Investig.* **119,** 1201–1215
31. Hunte, C., von Jagow, G., and Schagger, H. (2003) *Membrane Protein Purification and Crystallization. A Practical Guide*, 2nd Ed., Academic Press, New York
32. Bauer, A. J., Gieschler, S., Lemberg, K. M., McDermott, A. E., and Stockwell, B. R. (2011) Functional model of metabolite gating by human voltage-dependent anion channel 2. *Biochemistry* **50,** 3408–3410
33. Bose, H. S., Sugawara, T., Strauss, J. F., 3rd, Miller, W. L., and International Congenital Lipoid Adrenal Hyperplasia Consortium (1996) The pathophysiology and genetics of congenital lipoid adrenal hyperplasia. *N. Engl. J. Med.* **335,** 1870–1878
34. Lai, J. C., Tan, W., Benimetskaya, L., Miller, P., Colombini, M., and Stein, C. (2006) A pharmacologic target of G3139 in melanoma cells may be the mitochondrial VDAC. *Proc. Natl. Acad. Sci. U.S.A.* **103,** 7494–7499
35. Arakane, F., Sugawara, T., Nishino, H., Liu, Z., Holt, J. A., Pain, D., Stocco, D. M., Miller, W. L., and Strauss, J. F., 3rd (1996) Steroidogenic acute regulatory protein (StAR) retains activity in the absence of its mitochondrial targeting sequence: implications for the mechanism of StAR action. *Proc. Natl. Acad. Sci. U.S.A.* **93,** 13731–13736
36. Wang, X., Liu, Z., Eimerl, S., Timberg, R., Weiss, A. M., Orly, J., and Stocco, D. M. (1998) Effect of truncated forms of the steroidogenic acute regulatory (StAR) protein on intramitochondrial cholesterol transfer. *Endocrinology* **139,** 3903–3912
37. Hiller, S., Abramson, J., Mannella, C., Wagner, G., and Zeth, K. (2010) The 3D structure of VDAC represent a native conformation. *Trends Biochem. Sci.* **35,** 514–521
38. Rajapaksha, M., Kaur, J., Bose, M., Whittal, R. M., and Bose, H. S. (2013) Cholesterol-mediated conformational changes in the steroidogenic acute regulatory protein are essential for steroidogenesis. *Biochemistry* **52,** 7242–7253
39. Stern, J. B., and Jackson, R. C. (1985) Peptide products of the cleavage of bovine preprolactin by signal peptidase. *Arch. Biochem. Biophys.* **237,** 244–252
40. Bose, H. S., Whittal, R. M., Baldwin, M. A., and Miller, W. L. (1999) The active form of the steroidogenic acute regulatory protein, StAR, appears to be a molten globule. *Proc. Natl. Acad. Sci. U.S.A.* **96,** 7250–7255
41. Li, J. M., and Shore, G. C. (1992) Reversal of the orientation of an integral protein of the mitochondrial outer membrane. *Science* **256,** 1815–1817
42. Nicchitta, C. V., and Blobel, G. (1989) Nascent secretory chain binding and translocation are distinct processes: differentiation by chemical alkylation. *J. Cell Biol.* **108,** 789–795
43. Simmen, T., Lynes, E. M., Gesson, K., and Thomas, G. (2010) Oxidative protein folding in the endoplasmic reticulum: tight links to the mitochondria-associated membrane (MAM). *Biochim. Biophys. Acta* **1798,** 1465–1473
44. Capponi, A. M., Rossier, M. F., Davies, E., and Vallotton, M. B. (1988) Calcium stimulates steroidogenesis in permeabilized bovine adrenal cortical cells. *J. Biol. Chem.* **263,** 16113–16117
45. Kaufman, R. J. (1999) Stress signaling from the lumen of the endoplasmic reticulum: coordination of genes transcriptional and translational control. *Genes Dev.* **13,** 1211–1233
46. Ni, M., and Lee, A. S. (2007) ER chaperone in mammalian development and human diseases. *FEBS Lett.* **581,** 3641–3651
47. Rutkowski, D. T., and Hegde, R. S. (2010) Regulation of basal cellular physiology by the homeostatic unfolded protein response. *J. Cell Biol.* **189,** 783–794
48. Bose, H. S., Baldwin, M. A., and Miller, W. L. (1998) Incorrect folding of steroidogenic acute regulatory protein (StAR) in congenital lipoid adrenal hyperplasia. *Biochemistry* **37,** 9768–9775
49. Tsujishita, Y., and Hurley, J. H. (2000) Structure and lipid transport mechanism of a StAR-related domain. *Nat. Struct. Biol.* **7,** 408–414
50. Rosenfeld, J., Capdevielle, J., Guillemot, J. C., and Ferrara, P. (1992) In-gel digestion of proteins for internal sequence analysis after one- or two-dimensional electrophoresis. *Anal. Biochem.* **203,** 173–179